Deep congenic analysis identifies many strong, context-dependent QTLs, one of which, *Slc35b4*, regulates obesity and glucose homeostasis

Soha N. Yazbek,[1,3,5] David A. Buchner,[1,3,6] Jonathan M. Geisinger,[1] Lindsay C. Burrage,[1,7] Sabrina H. Spiezio,[1,8] Gabriel E. Zentner,[1] Chang-Wen Hsieh,[2] Peter C. Scacheri,[1] Colleen M. Croniger,[2,4] and Joseph H. Nadeau[1,4,8,9]

[1]*Department of Genetics, Case Western Reserve University School of Medicine, Cleveland, Ohio 44106, USA;* [2]*Department of Nutrition, Case Western Reserve University School of Medicine, Cleveland, Ohio 44106,USA*

Although central to many studies of phenotypic variation and disease susceptibility, characterizing the genetic architecture of complex traits has been unexpectedly difficult. For example, most of the susceptibility genes that contribute to highly heritable conditions such as obesity and type 2 diabetes (T2D) remain to be identified despite intensive study. We took advantage of mouse models of diet-induced metabolic disease in chromosome substitution strains (CSSs) both to characterize the genetic architecture of diet-induced obesity and glucose homeostasis and to test the feasibility of gene discovery. Beginning with a survey of CSSs, followed with genetic and phenotypic analysis of congenic, subcongenic, and subsubcongenic strains, we identified a remarkable number of closely linked, phenotypically heterogeneous quantitative trait loci (QTLs) on mouse chromosome 6 that have unexpectedly large phenotypic effects. Although fine-mapping reduced the genomic intervals and gene content of these QTLs over 3000-fold, the average phenotypic effect on body weight was reduced less than threefold, highlighting the "fractal" nature of genetic architecture in mice. Despite this genetic complexity, we found evidence for 14 QTLs in only 32 recombination events in less than 3000 mice, and with an average of four genes located within the three body weight QTLs in the subsubcongenic strains. For *Obrq2a1*, genetic and functional studies collectively identified the solute receptor *Slc35b4* as a regulator of obesity, insulin resistance, and gluconeogenesis. This work demonstrated the unique power of CSSs as a platform for studying complex genetic traits and identifying QTLs.

[Supplemental material is available for this article.]

The genetic architecture of complex traits and discovery of the underlying genes is fundamental to studies of phenotypic variation and disease risk. In particular, the identification of susceptibility genes and their interaction networks could define new protein and pathway targets for interventions. However, obesity and type 2 diabetes (T2D) each illustrate the progress and challenges in complex trait analysis. Although heritability estimates demonstrate the importance of genetic factors in disease risk (Stolerman and Florez 2009), and the discovered genes such as fat mass and obesity associated (*FTO*) have led to insights into disease pathogenesis (Gerken et al. 2007; Cecil et al. 2008), many large-scale studies of 10s of thousands of individuals collectively account for an unexpectedly modest fraction of the phenotypic variance (Manolio et al. 2009). Therefore, the nature of missing heritability remains to be determined (Manolio et al. 2009).

Many complications challenge studies of genetic architecture and identification of complex trait genes (quantitative trait loci [QTLs]), including genetic factors such as nonadditive interactions (epistasis), genetic heterogeneity, low penetrance, and transgenerational effects, as well as technical issues such as limited sample size and multiple testing penalties (Phillips 2008; Mackay et al. 2009; Manolio et al. 2009; Nadeau 2009; McClellan and King 2010). Model organisms have many advantages, including the ability to control environmental factors, conduct defined crosses, functionally evaluate candidate genes in vivo and in vitro, study multiple genetically identical individuals, and undertake rigorous mechanistic studies. Chromosome substitution strains (CSSs), which are a novel paradigm for studying complex traits, dramatically reduce multiple testing penalties while simultaneously facilitating the detection of QTLs with additive as well as epistatic effects (Shao et al. 2008). Congenic strains share these advantages with CSSs and can be generated following only four generations of breeding when derived from CSSs rather than 10 generations using conventional breeding methodologies, and like CSSs, they are permanent resources for genetic and functional studies of complex traits and models of human conditions (Nadeau et al. 2000; Shao et al. 2010).

Pilot studies of various blood, bone, and metabolic traits in CSSs and their congenic strains suggest a surprising picture of the genetic architecture of complex traits. In particular, these studies reveal a large number of QTLs with strong and nonadditive phenotypic effects (Matin et al. 1999; Nadeau et al. 2000; Youngren et al. 2003; Shao et al. 2008, 2010). For example, despite being only one of four QTLs on chromosome 6 and one of 19 QTLs across the genome affecting glucose homeostasis and adiposity, *Obrq2* (obesity resistance

[3]**These authors contributed equally to this work.**
[4]**These authors contributed equally to this work.**
Present addresses: [5]Faculty of Health Sciences, American University of Beirut, Beirut, Raid El-Solh 1107202, Lebanon; [6]Life Sciences Institute, University of Michigan, Ann Arbor, Michigan 48109, USA; [7]Department of Pediatrics, University Hospitals Case Medical Center, Cleveland, Ohio 44106, USA; [8]Institute for Systems Biology, Seattle, Washington 98109, USA.
[9]Corresponding author.
E-mail jnadeau@systemsbiology.org.
Article published online before print. Article, supplemental material, and publication date are at http://www.genome.org/cgi/doi/10.1101/gr.120741.111.

QTL-2) accounts for 65% of the body weight difference between the B6 and A/J parental strains (Buchner et al. 2008, 2010). However, it is unclear from these studies whether this complexity extends to finer levels of genetic resolution or instead simplifies to a more conventional model of QTLs with small, additive phenotypic effects. Resolving these questions of genetic architecture, missing heritability, and gene discovery is a major challenge in genetics.

Genetic and phenotypic complexity within the *Obrq2* locus

We selected *Obrq2* to evaluate the genetic and phenotypic complexity of a single QTL that affects diet-induced obesity and glucose homeostasis (Fig. 1A; Buchner et al. 2008, 2010). To dissect *Obrq2*, males from each of five subcongenic strains were derived from the 6C2 congenic strain and then evaluated for body weight after 100 d on a high-fat, simple carbohydrate (HFSC) diet (Fig. 1B). These five strains revealed four sub-QTLs that regulate diet-induced obesity (Fig. 1B). Identification of four distinct sub-QTLs assumes that the regions of A/J-derived and B6-derived sequence within the 10.37-Mb interval between rs13478699 and rs30569437 are identical in strains 6C2b (obese), 6C2c (lean), and 6C2d (lean). To test this assumption, these strains were genotyped with additional SNP markers within this interval. All three strains were found to have a single recombination event within a 240-kb interval between SNP markers rs30960190 and rs30221945 (Fig. 1C; data not shown), which strongly suggests that the genomic sequence of each strain differs only due to their proximal, and not distal, recombination breakpoints. Thus, these data support identification of four distinct QTLs. Surprisingly, while *Obrq2* accounts for a 7.17-g weight difference between the parental strains, the four sub-QTLs had phenotypic effects of similarly large magnitudes, conferring decreases of 6.04 g for $Obrq2a^{A/J}$, 5.93 g for $Obrq2c^{A/J}$, and 3.44 g for $Obrq2d^{A/J}$ and an increase of 5.35 g for $Obrq2b^{A/J}$. Strain 6C2d, which defines *Obrq2a*, had the largest effect on body weight and also showed a significantly reduced fasting insulin, glucose, and HOMA-IR relative to C57BL/6J (B6) males (Table 1). Additional SNPs narrowed *Obrq2a* to a 3.2-Mb interval between markers rs29927775 and rs30221945 (Supplemental Table S1), thereby reducing the number of genes from 216 to 19.

To evaluate the genetic and phenotypic complexity at *Obrq2a*, we generated eight subsubcongenic strains that together spanned the 3.2-Mb *Obrq2a* locus (Fig. 1C). Five-week old males of each strain were placed on the HFSC diet for 100 d, at which time their body weight was measured and glucose homeostasis assessed (Table 2). Within the *Obrq2a* interval that confers a 6.04-g difference in body weight, four subsub-QTLs were discovered that accounted for decreases of 3.55 g for $Obrq2a1^{A/J}$, 3.96 g for $Obrq2a4^{A/J}$, 5.34 g for $Obrq2a5^{A/J}$, and 3.83 g for $Obrq2a6^{A/J}$. Two additional subsub-QTLs were discovered that affect aspects of glucose homeostasis (*Obrq2a2* for fasting glucose and *Obrq2a3* for fasting glucose, fasting insulin, and HOMA) with no significant effect on body weight (Fig. 1; Table 2). Remarkably, each of the six subsub-QTLs controlled distinct combinations of traits, often uncoupling the usual association between obesity and glucose homeostasis (Fig. 2; Table 2). Thus, a single QTL in congenic strains revealed four sub-QTLs in subcongenic strains and one of these revealed six

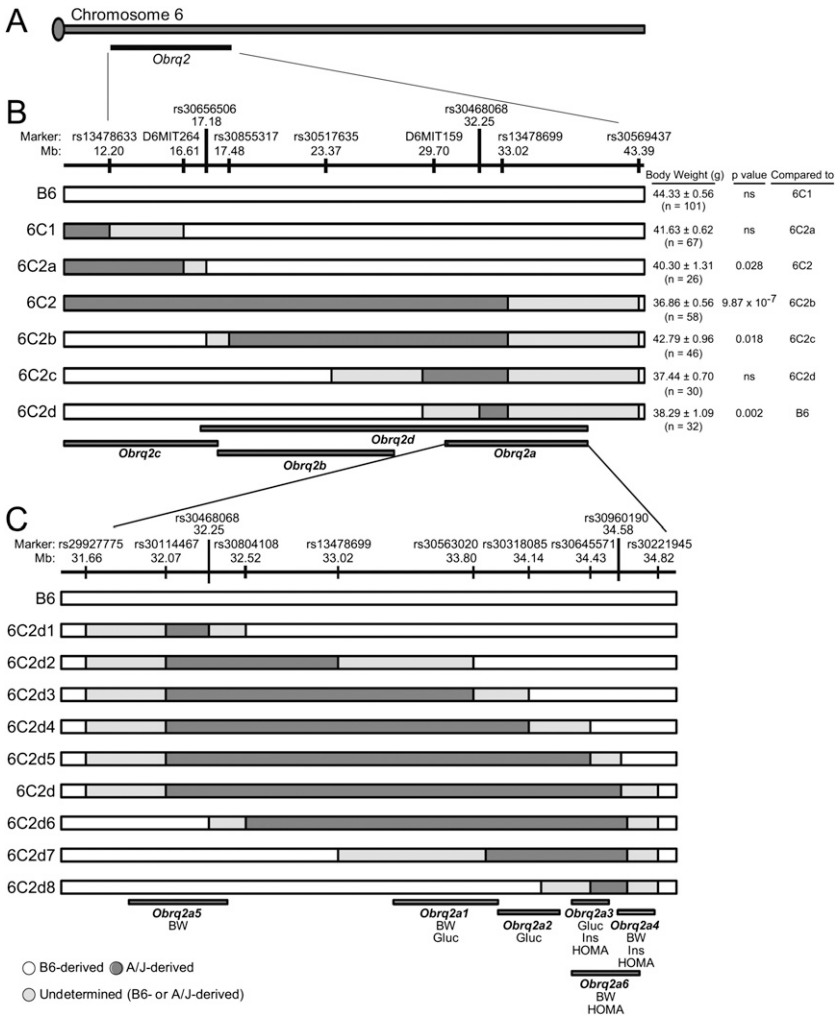

Figure 1. Schematic of subcongenic and subsubcongenic strains derived from strain 6C2 and 6C2d. (*A*) The location of *Obrq2* is indicated relative to chromosome 6. Map of chromosome 6 subcongenic (*B*) and subsubcongenic (*C*) panels that define QTLs for body weight and measures of insulin resistance. *Obrq2* is located in a 30.3-Mb interval between markers rs13478633 and rs30218447 that differs genetically between the 6C1 obesity-susceptible and 6C2 obesity-resistant congenic strains (see also panel *B*) (Buchner et al. 2010). Strain names are indicated on the *left*. Body weight data are presented as mean ± SEM. An asterisk indicates statistical significance ($P < 0.05$) following adjustment for Bonferroni correction. QTL intervals are arbitrarily drawn with the proximal and distal boundaries halfway between the flanking markers. (BW) QTL regulates body weight; (Gluc) QTL regulates fasting glucose levels; (Ins) QTL regulates fasting insulin levels. The overlap between *Obrq2d* with both *Obrq2a* and *Obrq2c* as well as *Obrq2a6* with both *Obrq2a3* and *Obrq2a4* may indicate a common genetic basis for the overlapping QTLs rather than distinct QTLs.

Table 1. Metabolic properties of strains B6 and 6C2d that define *Obrq2a*

Strain	Body weight (g)	Glucose (mg/dl)	Insulin (μg/L)	HOMA-IR
B6	44.33 ± 0.56 (*n* = 101)	185.3 ± 12.5 (*n* = 19)	1.06 ± 0.2 (*n* = 19)	13.6 ± 2.9 (*n* = 19)
6C2d	38.29 ± 1.09[a] (*n* = 32)	142 ± 5.6[a] (*n* = 19)	0.36 ± 0.05[a] (*n* = 18)	2.0 ± 0.4[a] (*n* = 18)

Data presented as mean ± SEM.
[a]$P < 0.005$ after Bonferroni correction.

phenotypically heterogeneous subsub-QTLs in subsubcongenic strains, but the magnitude of their phenotypic effects on body weight remained remarkably similar across these markedly different levels of genetic resolution.

Fractal genetics of complex traits

Next we focused on the genetic architecture of diet-induced obesity resistance and insulin resistance by taking advantage of the genetic and phenotypic information at progressively finer levels of genetic resolution, namely, chromosome substitution, congenic, subcongenic, and subsubcongenic strains. We found a striking and definitive pattern over the 3000-fold difference in resolution, with multiple QTLs that have strong but context-dependent phenotypic effects (Fig. 1). Presumably most eluded discovery previously because of their close linkage and contrasting phenotypic effects (Burrage et al. 2010). For example, the neighboring *Obrq2a3* and *Obrq2a4* QTLs have strong but counter-balancing effects on fasting insulin levels and were only detected because of the recombination breakpoint in strain 6C2d5 (Fig. 1C). Because detection depends heavily on the number of congenic strains analyzed, the true number of QTLs and their interactions is probably underestimated.

Next we systematically characterized the number and physical size of QTLs, number of genes within the QTL intervals, and magnitude of the phenotypic effect for body weight at each level of genetic resolution (Table 3). The overall genetic variation between B6 and A/J mice is associated with an 11.09-g difference in body weight after 100 d on the HFSC diet, whereas CSSs account for an average weight difference of 8.36 g, despite only containing on average of 4.4% of the A/J genome and an average of 1485 genes (Singer et al. 2004). The chromosome 6 substitution strain is typical of this general pattern, accounting for a 9.55-g weight difference while containing only 5.5% of the A/J-genome and 1906 genes. The congenic, subcongenic, and subsubcongenic strains that carry increasingly smaller segments of A/J-derived chromosome 6 account for differences in average body weight of 6.37 g (Shao et al. 2008), 5.77 g, and 4.28 g despite containing only 1%, 0.5%, and 0.03% of the A/J genome and including on average 342, 135, and four genes, respectively. Therefore, the magnitude of phenotypic effects did not decrease proportionally with the size of the QTL interval or the number of genes, a property that further supports and extends the description of genetic complexity underlying phenotypic variation as "fractal" (Kruglyak 2008).

The surprising finding that with finer genetic resolution the QTL effects on body weight remained large relative to the decreasing physical size of QTL intervals and the increasing number of QTLs identified, led us to perform replicate studies with selected strains at each level of resolution to both confirm QTL locations and test whether an ascertainment bias was responsible for the large effects on body weight. All strains were tested as before, with body weight measured in male mice following 100 d on the HFSC diet. In these replication studies, the congenic strain 6C1 (42.73 g ± 0.64, $n = 80$) weighed 8.18 g more than the congenic strain 6C2 (35.84 g ± 0.46, $n = 80$, $P < 0.0001$), which confirms the location of *Obrq2* and demonstrates a similar effect on body weight to that observed in the original study (6.12 g) (Fig. 1). Similarly, the subcongenic strain 6C2d (36.12 g ± 0.62, $n = 68$) (Table 1)weighed 8.58 g less than the B6 control strain (44.70 g ± 0.70, $n = 77$, $P < 0.0001$) (Table 2), which confirms the location of *Obrq2a* and also demonstrates a similar effect on body weight to that observed in the original study (6.04 g) (Fig. 1). Finally, the subsubcongenic strain 6C2d1 (39.82 g ± 1.62, $n = 17$) weighed 4.78 g less than the control strain B6 (44.60 ± 0.77 g, $n = 58$, $P < 0.006$), which confirms the location of *Obrq2a5* and again demonstrates a similar effect on body weight to that observed in the original study (2.68 g) (Fig. 1). Therefore, replicate studies at each level of genetic resolution together provide additional evidence for the validity of QTLs discovered in this study and suggest that the size of the effect on body weight is due to genetic variation within the QTL interval rather than an ascertainment bias.

To test whether the fractal phenomenon was specific to *Obrq2* or represented a more general feature of complex traits, an independent panel of six subcongenic strains was generated that spanned a 13.8-Mb region at the *Obrq1* QTL interval between SNP markers rs30950898 and D6CWRU1 (Supplemental Fig. 1; Shao et al. 2008). This interval is >50 Mb distal to *Obrq2*. Analysis of male body weight following 100 d on the HFSC diet revealed three QTLs, each of which had large and contrasting phenotypic effects similar to

Table 2. QTLs for body weight and insulin resistance in subsubcongenic strains 6C2d1-8 derived from subcongenic strain 6C2d

Strain	Body weight(g)	Glucose (mg/dl)	Insulin (μg/L)	HOMA-IR	Compared to
B6	44.70 ± 0.70 (*n* = 77)	185.3 ± 12.5 (*n* = 19)	1.06 ± 0.2 (*n* = 19)	13.6 ± 2.9 (*n* = 19)	6C2d-1
6C2d-1	42.02 ± 0.67 (*n* = 71)	192.4 ± 8.2 (*n* = 28)	0.76 ± 0.08 (*n* = 27)	9.06 ± 1.4 (*n* = 27)	6C2d-2
6C2d-2	**42.16 ± 0.88[a] (*n* = 43)**	**191.5 ± 7.7[a] (*n* = 32)**	0.85 ± 0.12 (*n* = 24)	11.18 ± 2.1 (*n* = 24)	6C2d-3
6C2d-3	38.61 ± 0.87 (*n* = 32)	**156.9 ± 5.5[b] (*n* = 37)**	0.53 ± 0.06 (*n* = 29)	5.62 ± 0.7 (*n* = 29)	6C2d-4
6C2d-4	41.90 ± 1.03 (*n* = 32)	**126.1 ± 8.0[a] (*n* = 22)**	**0.45 ± 0.08[a] (*n* = 19)**	**5.90 ± 2.0[a] (*n* = 19)**	6C2d-5
6C2d-5	**40.08 ± 0.90[b] (*n* = 41)**	172.5 ± 15.2 (*n* = 20)	**0.71 ± 0.11[a] (*n* = 19)**	**9.47 ± 2.0[a] (*n* = 19)**	6C2d
6C2d	**36.12 ± 0.62[b] (*n* = 68)**	142 ± 5.6 (*n* = 19)	0.36 ± 0.05 (*n* = 18)	2.0 ± 0.4 (*n* = 18)	6C2d-6
6C2d-6	41.46 ± 0.85 (*n* = 47)	162 ± 8.1 (*n* = 29)	0.46 ± 0.08 (*n* = 27)	6.91 ± 1.6 (*n* = 27)	6C2d-7
6C2d-7	39.91 ± 1.10 (*n* = 28)	193.3 ± 9.2 (*n* = 31)	0.74 ± 0.09 (*n* = 29)	9.66 ± 1.4 (*n* = 29)	6C2d-8
6C2d-8	**40.87 ± 0.67[b] (*n* = 76)**	195.3 ± 8.2 (*n* = 31)	0.71 ± 0.08 (*n* = 34)	**8.45 ± 1.2[a] (*n* = 31)**	B6

Progenitor strains are highlighted in gray, and significant differences are highlighted in bold. Data presented as mean ± SEM.
[a]$P < 0.05$ after Bonferroni correction.
[b]$P < 0.005$ after Bonferroni correction.

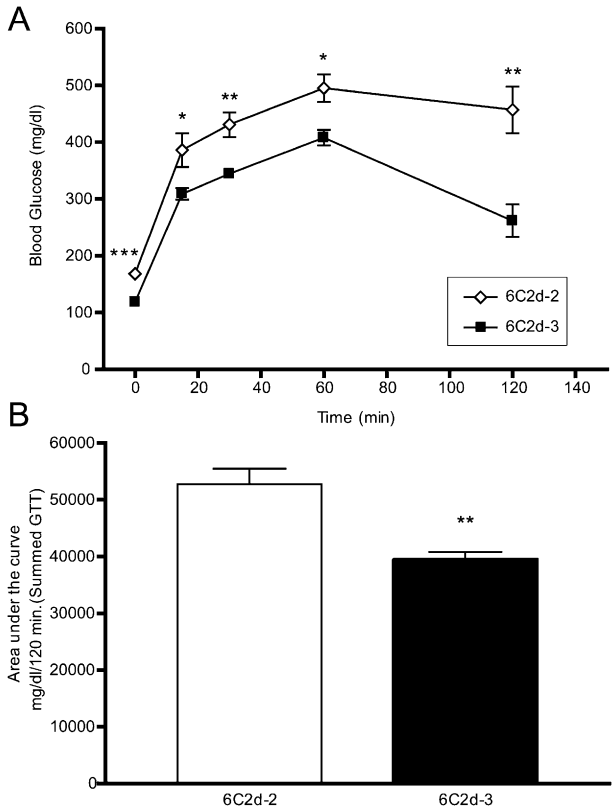

Figure 2. Strain 6C2d-2 has increased fasting glucose levels and decreased glucose tolerance compared to 6C2d-3. (*A*) Glucose levels were measured 15, 30, 60, and 120 min following an IP injection of glucose (n = 8). (*B*) Area under the curve (AUC) was calculated by summing the integration values of consecutive linear segments of the glucose curve shown in panel *A*. *P < 0.05, **P < 0.01, and ***P < 0.001.

those identified at *Obrq2*. The three QTLs accounted for body weight changes of 5.91 g, 4.41g, and 2.97 g despite containing only 0.09%, 0.07%, and 0.14% of the A/J genome and including seven, three, and 20 genes, respectively. Given the limited statistical power to detect small phenotypic effects in this and other QTL studies, the average QTL phenotypic effect is usually overestimated. Nevertheless, we found many large effect QTLs, especially compared with those detected in other QTL mapping paradigms. Analysis of additional CSSs and congenic strains suggests that other traits and chromosomes show similar genetic architectures, in terms of QTL number, context-dependence, and strong phenotypic effects (Youngren et al. 2003; Shao et al. 2008; Millward et al. 2009). Whether this genetic complexity compromises gene discovery is an open question.

Improved glucose tolerance at *Obrq2a1*

To test the feasibility of gene discovery in a fractal genome, we focused on *Obrq2a1* (defined by markers rs1348699 and rs30318085) because it regulates body weight and fasting glucose levels and because it contains the fewest number of genes (three) among the QTLs identified. Measurement of fasting glucose levels suggests a disruption of glucose homeostasis on subcongenic strains 6C2d-2 and 6C2d-3 (Table 2). To characterize the dynamics of glucose metabolism more rigorously, a glucose tolerance test (GTT) showed a reduced fasting glucose level in strain 6C2d-3 and significantly reduced plasma glucose levels at all timepoints following a bolus intraperitoneal (IP) injection of glucose (Fig. 2A). Reduced glucose levels in 6C2d-3 correspond to an ~25% decline throughout the tolerance curve (Fig. 2B). Thus, strain 6C2d-3 with $Obrq2a1^{A/J}$ exhibited reduced tolerance to glucose relative to strain 6C2d-2 with $Obrq2a1^{B6}$.

Decreased gluconeogenesis due to improved hepatic insulin sensitivity at *Obrq2a1*

To identify the cause of the disruption of glucose homeostasis associated with *Obrq2a1*, a hyperinsulinemic-euglycemic clamp was performed on strains 6C2d-2 and 6C2d-3 to test insulin sensitivity and tissue-specific glucose uptake. These strains were maintained at equivalent and physiologically normal plasma glucose levels throughout the experiment (Fig. 3A). 6C2d-3 required a higher glucose infusion rate (GIR) relative to 6C2d-2 to maintain euglycemia under hyperinsulinemic conditions (Fig. 3B). Therefore, $Obrq2a1^{A/J}$ in 6C2d-3 is associated with increased insulin sensitivity. The glucose clearance rate and glucose uptake in peripheral tissue did not differ between the two strains (Fig. 3C,E,F). The difference in GIR is therefore due to a decrease in endogenous glucose production and not to differences in glucose uptake (Fig. 3D). Thus, the relative improvement in the ability to shut down de novo gluconeogenesis demonstrates that $Obrq2a1^{A/J}$ enhances hepatic sensitivity to insulin.

Candidate gene analysis of the *Obrq2a1* interval

We next analyzed DNA sequence and measured gene expression levels for the three genes located at *Obrq2a1* (Ensembl version 56). Exocyst complex component 4 (*Exoc4*, alias *Sec8*) encodes a protein that is part of the octameric exocyst complex (Saito et al. 2008). Decreased expression of *Exoc4* blocks insulin-stimulated glucose uptake (Inoue et al. 2006) by inhibiting SLC2A4 (solute carrier family 2 [facilitated glucose transporter], member 4 [GLUT4]) docking at the plasma membrane (Lyons et al. 2009). The second gene is leucine-rich repeats and guanylate kinase domain containing (*Lrguk*), a gene with no known function. The third gene is solute carrier family 35, member B4 (*Slc35b4*), which is localized in the golgi membrane, where it facilitates transport of UDP-xylose and UDP-*N*-acetylglucosamine into the golgi (Ashikov et al. 2005). DNA sequence differences between B6 and A/J were not found within the coding or untranslated regions of these genes or in any of the evolutionarily conserved noncoding sequence blocks within the *Obrq2a1* interval (Ensembl v56) (data not shown).

Table 3. Summary of QTL effects on body weight at different levels of genetic resolution

Strains	No. of QTLs	QTL size (Mb)	% of genome	No. of genes	Difference in body weight (g)
Parental	1	2717.0	100	22,974	11.09
CSS	16	120.3 ± 9.0	4.4 ± 0.3	1485 ± 155	8.36 ± 0.49
Congenic	4	27.6 ± 7.8	1.0 ± 0.3	342 ± 66	6.37 ± 1.04
Subcongenic	6	8.6 ± 2.7	0.3 ± 0.1	73 ± 33	5.10 ± 0.49
Subsubcongenic	3	0.8 ± 0.2	0.03 ± 0.01	4 ± 1	4.28 ± 0.54

The genetic composition of the congenic strains prevented testing for nonadditive interactions because most QTLs were studied in combination rather than independently.

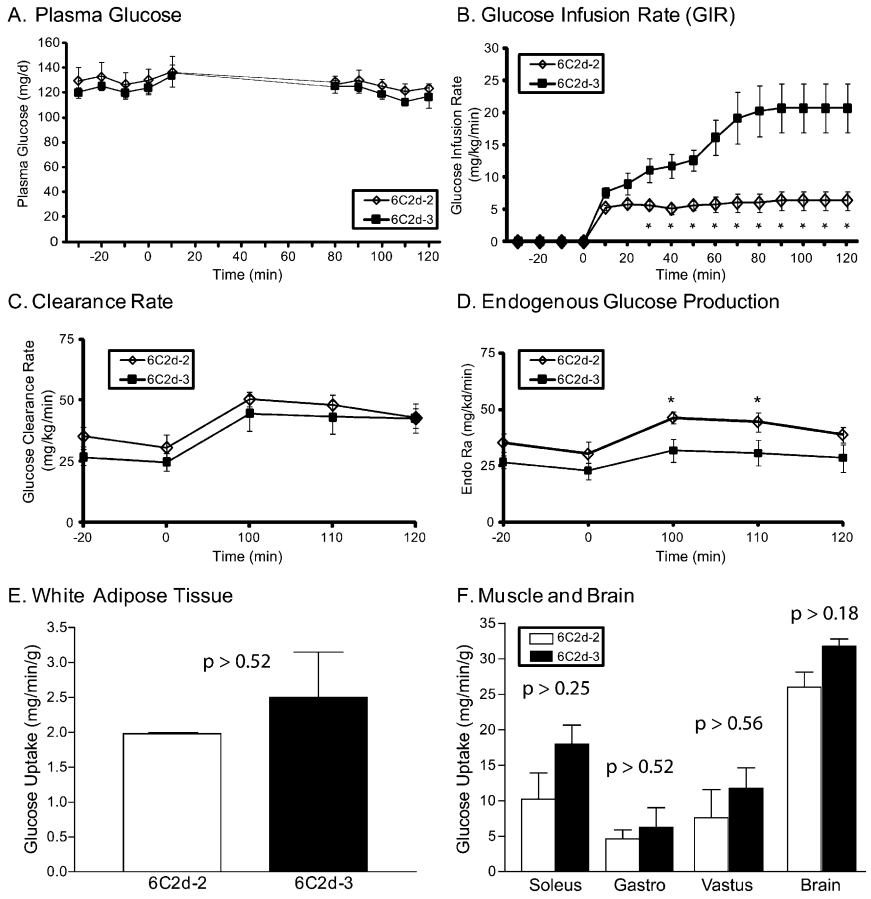

Figure 3. 6C2d-2 is insulin resistant relative to 6C2d-3. (*A*) Plasma glucose levels were maintained at constant levels throughout the hyperinsulinemic-euglycemic clamp study. (*B*) Increased glucose infusion rate required to maintain euglycemia in strain 6C2d-3 relative to strain 6C2d-2. (*C*) Glucose clearance rate (Rd) did not differ between strains 6C2d-2 and 6C2d-3, indicating that (*D*) endogenous glucose production was increased in strain 6C2d-2. Glucose uptake in (*E*) muscle, brain and (*F*) white adipose tissue (WAT) did not differ between the two strains. Data are presented as mean ± SEM. **P* < 0.05.

We then measured the relative mRNA expression levels for each of the three genes in physiologically relevant tissues (liver, muscle, pancreas, and white adipose) (Table 4). *Lrguk* mRNA was not detected in the pancreas and was found at low levels in the other tissues, consistent with evidence that *Lrguk* is primarily expressed in testes (Wu et al. 2009). Moreover, expression of both *Exoc4* and *Lrguk* did not differ in any of the tissues analyzed between the two strains that define *Obrq2a1*. Given the role of *Exoc4* in glucose uptake, these data are consistent with the observation that glucose uptake did not differ between strains 6C2d-2 and 6C2d-3 (Fig. 3E,F). Interestingly, *Slc35b4* expression in the liver was 1.5-fold higher in strain 6C2d-2 relative to strain 6C2d-3 ($P < 0.05$) but did not differ in the other tissues examined. Thus, *Slc35b4* is the only gene within the QTL interval with an expression level difference among the tissues surveyed. We therefore propose that altered hepatic expression of *Slc35b4* controls hepatic insulin resistance and gluconeogenesis associated with *Obrq2a*.

SLC35B4 regulates glucose synthesis

To directly test whether SLC35B4 is involved in hepatic glucose production, glucose synthesis was measured in H2.35 (mouse, liver-derived) and HepG2 (human, hepatoma-derived) cells transfected either with a control nontargeting siRNA or with a siRNA against *Slc35b4*. Levels of *Slc35b4* mRNA were reduced more than 50% after siRNA targeting in both cell lines (Fig. 4A,C), which is greater than the 50% difference in expression level between the congenic strains 6C2d-2 and 6C2d-3 that define *Obrq2a1* (Table 4). Knockdown of *Slc35b4* in H2.35 cells decreased glucose production by 35% (Fig. 4B), demonstrating that a reduction in *Slc35b4* mRNA levels is sufficient to decrease glucose synthesis. This is consistent with the decreased expression of *Slc35b4* playing a causative role in the reduction in hepatic gluconeogenesis in the strain 6C2d-3 relative to 6C2d-2. Interestingly, the HepG2 cell culture experiments demonstrate that decreased *SLC35B4* expression led to increased gluconeogenesis (Fig. 4D), whereas both the mouse in vivo and in vitro studies found that decreased *Slc35b4* expression is associated with decreased gluconeogenesis (Table 4; Figs. 3, 4). Whether this difference is attributable to a species difference or to the unique metabolic properties of the carcinoma-derived HepG2 cells remains to be determined.

Discussion

We report the first use of CSSs and congenic, subcongenic, and subsubcongenic strains to study genetic architecture and to establish the identity of complex trait genes. We found a striking and

Table 4. Quantitative RT-PCR analysis of *Obrq2a1* candidate genes

	Muscle		Liver		Pancreas		White adipose	
Gene	6C2d-2	6C2d-3	6C2d-2	6C2d-3	6C2d-2	6C2d-3	6C2d-2	6C2d-3
Slc35b4	1.0 ± 0.1	4.2 ± 1.4	**1.5 ± 0.1**	**1.0 ± 0.1**[a]	1.7 ± 1.1	1.0 ± 0.9	1.0 ± 0.2	1.1 ± 0.1
Lrguk	1.0 ± 0.2	1.2 ± 0.3	1.0 ± 0.1	1.3 ± 0.2	ND	ND	1.2 ± 0.2	1.0 ± 0.1
Exoc4	1.0 ± 0.2	1.3 ± 0.1	1.6 ± 0.3	1.0 ± 0.1	1.0 ± 0.2	3.6 ± 2.0	1.0 ± 0.2	1.0 ± 0.1

Data presented as mean ± SEM, $n = 5$–6 per group. ND indicates not detected. Significant *P*-value is indicated in bold.
[a]$P < 0.05$ relative to 6C2d-2 after Bonferroni correction.

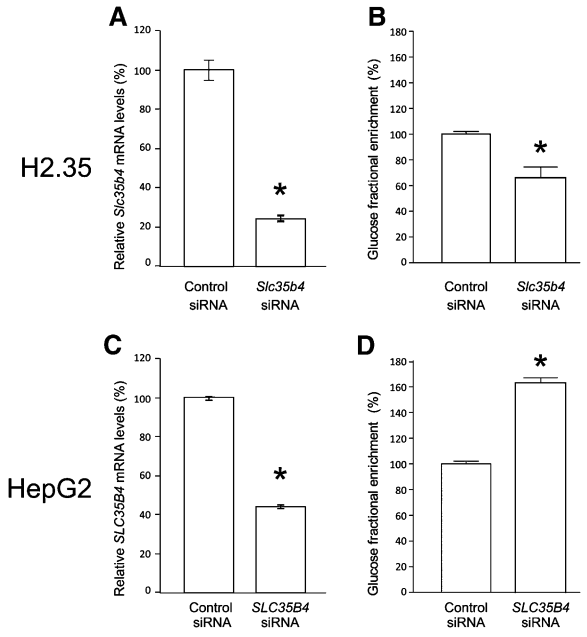

Figure 4. SLC35B4 regulates gluconeogenesis. *Slc35b4* mRNA levels (*A*,*C*) and glucose synthesis (*B*,*D*) were measured following transfection of H2.35 mouse liver-derived cells (*A*,*B*) or human hepatoma-derived HepG2 cells (*C*,*D*), with either a nontargeting siRNA (control) or an siRNA targeting *Slc35b4*. Levels of mRNA and glucose synthesis were measured 48 h post transfection. Data are presented as mean ± SEM. **P* < 0.05 relative to control siRNA.

definitive pattern over the 3000-fold difference in resolution, from the entirety of the A/J genome to QTLs that average just 800 kb in subsubcongenic strains, with multiple QTLs that have strong phenotypic effects, suggesting a genetic architecture at odds with that which has frequently been proposed for humans, mice, and other model organisms, where phenotypic variation and risk for common diseases is thought to result from the cumulative action of hundreds of genes with small and additive effects (Flint and Mackay 2009; Gibson 2009; Mackay et al. 2009). It is remarkable that a single chromosome can harbor at least 14 QTLs for a single trait, each of which accounts for approximately half of the phenotypic difference between the parental strains. Interestingly, although the QTLs discovered in these studies may each regulate body weight, inclusion of other phenotype information such as measures of insulin resistance revealed the phenotypically unique nature of each QTL (Table 2; Fig. 2C), suggesting that QTL analysis may benefit from detailed phenotyping to distinguish related but distinct phenotypes (Fig. 1; Table 3; Kruglyak 2008).

The context-dependent nature of the QTLs identified with congenic analysis may contribute to their difficulty of detection in linkage and association studies (Kruglyak 2008). Our study discovered many QTLs with large phenotypic effects that were heavily dependent on genetic background. For example, *Obrq2a5*$^{A/J}$ confers obesity resistance in strain 6C2d (relative to strain 6C2d6) but has no effect in strain 6C2d2 (relative to B6) (Fig. 1C; Table 2). Similarly, *Obrq2a1*$^{A/J}$ confers obesity resistance in strain 6C2d3 (relative to 6C2d2) but has no effect in strains 6C2d6 and 6C2d7 (one or both of which carry *Obrq2a1*$^{A/J}$) that do not differ from 6C2d8 with respect to body weight (Fig. 1C; Table 2). Further investigation is required to test whether the context dependence observed here, presumably due to the large numbers of interacting loci, results from artificial selection applied during inbreeding or is also found in natural populations of mice and humans. In humans, these features would appear as incomplete penetrance. Interestingly, GWAS have had recent success identifying low penetrance susceptibility alleles for genetically complex disease (Meijers-Heijboer et al. 2002; Emison et al. 2005; Renwick et al. 2006; Seal et al. 2006; Erkko et al. 2007; Rahman et al. 2007; Brown et al. 2008; Brunetti-Pierri et al. 2008; Di Bernardo et al. 2008; Tomlinson et al. 2008; Papaemmanuil et al. 2009). Although the benefits of additional genome-wide association studies (GWAS) have recently been questioned (Goldstein 2009; McClellan and King 2010), our data suggest that additional power will result in the identification of common, but context-dependent, risk alleles. Importantly, because of context dependence, these risk alleles will have low odds ratios for the population but nonetheless may have large effects on an individual basis.

In addition to the difficulty in mapping traits due to the strong influence of genetic background, the large number of tightly linked QTLs with contrasting effects likely contributes to the difficulty in identifying complex trait genes. For instance, QTLs identified using a traditional mouse cross typically have a 95% confidence interval that spans ~30 Mb (Mott and Flint 2008). A recent study in yeast suggests that the low resolution of QTL interval mapping for complex traits can be overcome by dramatically increasing the number of recombination events analyzed (Ehrenreich et al. 2010), although the scale (10^7 recombinants were examined to identify one to 25 QTLs per trait) is prohibitive for studies of vertebrate model systems. In contrast, we identified 14 QTLs by thoroughly evaluating only 32 recombination events. Less than 3000 mice were used to generate both the *Obrq2a* subsubcongenic panel and the *Obrq1* subcongenic panel; therefore, a single laboratory can efficiently use the CSS and congenic paradigm for gene identification of complex traits in a mammalian model organism. Additionally, despite the genetic complexity of metabolic disease highlighted by studies of CSSs and their congenic strains, QTL discovery is highly feasible and efficient, as shown by the identification of *Slc35b4* as a regulator of obesity, insulin resistance, and gluconeogenesis. Similar candidate gene analysis could easily be applied for gene identification for the other 13 QTLs identified in these congenic strains.

Identifying the genetic factors affecting obesity and diabetes susceptibility opens a window into the molecular pathophysiology of disease (Altshuler et al. 2008). Variation in hepatic *Slc35b4* expression and altered hepatic gluconeogenesis together suggest that a liver autonomous defect is responsible for the hepatic insulin resistance. *Slc35b4* encodes a protein that transports UDP-xylose and UDP-*N*-acetylglucosamine from the cytosol into the golgi and may therefore alter the bioavailability of its cargo nucleotide sugars for post-translational modification (Ashikov et al. 2005). More than 600 proteins, including the insulin receptor IRS1, NOTCH, AKT, and AMPK, are modified with the addition of an UDP-xylose or UDP-*N*-acetylglucosamine moiety and may therefore contribute to the pleiotropic presentation of T2D and insulin resistance (Love and Hanover 2005; Yang et al. 2008; Teo et al. 2010). Interestingly, a SNP in the human *SLC35B4* gene (rs1619682) is associated with waist circumference (Fox et al. 2007), and chromosome 7q33, where *SLC35B4* is located, is associated with variation in body mass index (BMI), metabolic syndrome, fasting glucose, pro-insulin levels, and fat stores (Arya et al. 2002; Feitosa et al. 2002; Tang et al. 2003; Saunders et al. 2007; Laramie et al. 2008).

In summary, the study of CSSs and derived congenic strains has identified that *Slc35b4* regulates obesity and glucose homeostasis, as well as identified many additional QTLs with similarly large effects on metabolic traits, any of which are suitable for further physiological

and genetic studies. Therefore, in contrast to other methods for complex trait analysis in mice (Aylor et al. 2011), CSSs represent a currently available model that can be used in a single laboratory and location (Wahlsten et al. 2003) to identify numerous large-effect QTLs with a suitable genetic resolution that allows for efficient candidate gene analysis and gene discovery.

Methods

Husbandry

B6 and congenic mice were obtained from breeding colonies at Case Western Reserve University and maintained as described (Buchner et al. 2008). Mice were fed Labdiet 5010 chow (PMI Nutrition International) until they were 5 wk of age, at which time male mice were fed a HFSC diet (D12331; Research Diets) for 16 wk. Mice had access to food and water ad libitum. All animal study protocols were approved by the Institutional Animal Care and Use Committee of Case Western Reserve University.

Generation of subcongenic and subsubcongenic strains

One panel of subcongenic strains was derived from strain 6C2 and one was derived from strain 6C7, and a panel of subsubcongenic strains was derived from strain 6C2d (Fig. 1). A similar breeding strategy was used to generate each panel. 6C2, 6C7, and 6C2d mice were each initially crossed to B6 mice. The resulting (6C2 × B6) F1, (6C7 × B6) F1, and (6C2d × B6) F1 mice were backcrossed to B6. N2F1 offspring were genotyped for polymorphic markers (Supplemental Table S1) to identify mice carrying a recombinant chromosome. The recombinant N2F1 mice were again backcrossed to B6, and the offspring that were heterozygous for the recombinant chromosome were intercrossed to homozygose the A/J-derived segment. Once homozygosed, brother–sister mating was used to maintain the congenic strains.

Sequence analysis

Evolutionary conserved noncoding sequence blocks were identified using the phastCons program that is available as part of the UCSC Genome Browser (Siepel et al. 2005). SNPs between A/J and B6 within the *Obrq2a* interval were obtained from the Ensembl genome browser and compared to the phastCons sequence to determine if the SNPs were located within a conserved sequence block. TranscriptSNPView (Cunningham et al. 2006), which is incorporated in the Ensembl genome browser, was used to search for sequence variants between B6 and A/J within the coding region of *Slc35b4*, *Exoc4*, and *Lrguk*. Exons for which the complete sequence was not available from both B6 and A/J were analyzed by direct sequencing of B6 and A/J genomic DNA.

Measurements of insulin resistance

Fasting insulin and glucose levels were measured following 16 wk on the HFSC diet in male mice that were fasted overnight (16–18 h). The mice were anesthetized using isoflurane, and blood was collected from the retro-orbital sinus using a heparin coated capillary tube (Iris Sample Processing) into an EDTA-coated microtainer (Becton Dickinson). Glucose was measured from whole blood using a hand-held glucometer (OneTouch Ultra, Lifespan). Insulin was measured using a mouse ultra-sensitive ELISA kit (Mercodia). Homeostasis model assessment (HOMA) of insulin resistance was calculated using glucose and insulin measurements obtained using the following formula: [fasting glucose (mmol/L)] × [fasting insulin (μU/mL)]/22.5 (Plank et al. 2006). GTTs were performed on mice that were fasted overnight (16–18 h). Glucose was measured from tail blood with a hand-held glucometer at time 0 and at 15, 30, 60, and 120 min after an IP injection of dextrose dissolved in water (2 g/kg body weight). Hyperinsulinemic-euglycemic clamp procedures were done in the Case Western Reserve University Mouse Metabolic Phenotyping Center (MMPC) in awake, precatheterized, unrestrained, unanesthetized mice as described (Ayala et al. 2006). Determination of glucose uptake in peripheral tissues was performed with 2-deoxy-D-[1, 2-^{3}H] glucose as described (Halseth et al. 1999).

Tissue collection and RNA extraction

Mice were euthanized with a CO_2 overdose. Liver, pancreas, epididymal-fat pad, and hind-limb muscle tissue were collected and immediately placed in RNAlater (Ambion). RNA was extracted using an RNeasy mini-kit with RNase-free DNase treatment (Qiagen).

Real-time quantitative PCR

cDNA was synthesized from 2 μg of total RNA using the SuperScript III kit (Invitrogen). Taqman assays 00480588, 00262446, 00486020, and 01166707 were used respectively for *Slc35b4* (mouse), *SLC35B4* (human), *Exoc4*, and *Lrguk*. QPCR was performed as previously described (Hill-Baskin et al. 2009). Gene expression levels were calculated relative to the 18S rRNA control (TaqMan assay 004319413E) using the $2^{-\Delta\Delta Ct}$ calculation.

Cell culture

HepG2 cells were cultured in DMEM media (pH 7.4; Invitrogen) supplemented with gentamicin and 10% (v/v) fetal bovine serum (FBS) and maintained at 37°C in an atmosphere of 5% CO_2 and 95% air. H2.35 cells were cultured in DMEM media (pH 7.4) supplemented with gentamicin, 4% (v/v) FBS, and 250 nM dexamethason and were maintained at 33°C in an atmosphere of 5% CO_2 and 95% air. Cells were plated in six-well plates at a density of 1.0×10^5 cells/well and grown for 24 h. Transfection was performed according to the manufacturer's instructions (Dharmacon) using 2 μL of DharmaFECT-1 and a 100 nM per well final siRNA concentration (*SLC35B4* [Human] ON-TARGET plus SMART pool [L-007545-02]; *Slc35b4* [Mouse] ON-TARGET plus SMART pool [L-048155-01]; ON-TARGET plus nontargeting pool [D-001810-10]). HepG2 cells were treated with transfection reagent for 24 h, then rinsed with PBS, given fresh DMEM, and cultured for another 24 h. The medium was then removed and replaced with DMEM containing [U-^{13}C]glutamine or ^2H_2O to measure glucose synthesis. Total RNA was isolated 48 h post transfection (initial time-point for glucose assay) and analyzed by qRT-PCR.

Stable isotope measurement of glucose synthesis

Cells were incubated with [U-^{13}C]glutamine (HepG2) or ^2H_2O (H2.35) in the absence of glucose to measure the rates of gluconeogenesis. Cells were grown and transfected as described above and then incubated in glucose-free and 10% stripped FBS RPMI 1640 media that contained either 2. 5 mM [U-^{13}C]glutamine-enriched 100% MPE or 10% ^2H_2O. Case MMPC measured the synthesis of glucose from the cells and analyzed as the percentage of ^{13}C-label incorporation or ^{2}H-label incorporation into glucose by gas-chromatography. Briefly, 3 mL of chloroform-methanol mix (2:1, v/v) was added, and cells were homogenized. Layers were separated by water, and the chloroform layer was removed following centrifugation. To determine the percentage of glucose production, an aliquot of the aqueous layer was first evaporated to dryness and then converted to ^{13}C-labeled or ^{2}H-labeled penta-acetate derivative of glucose as

described previously with modifications (Previs et al. 1994). This was done by first reacting with hydroxylamine (20 mg/mL) in pyridine for 2 h at 80°C, and after cooling, 200 μL of acetic anhydride was added and further heated for 2 h at 60°C. The gas chromatography-mass spectrometry–derivatized samples were analyzed using an Agilent 5973N-MSD mass spectrometer equipped with an Agilent 6890 gas chromatograph with a DB17-MS capillary column (30 m × 0.25 mm × 0.25 μm). The mass spectrometer was operated in chemical ionization (CI) mode with ammonia gas. Gas chromatographic conditions were as follows: 1 μL sample was injected in split-less mode (inlet heated to 270°C) at the initial 100°C. The oven was ramped at 20°C/min until 300°C; selective ion monitoring for 405–408 m/z was performed. For example, for unlabeled MO, 405 ion was monitored, and for labeled "M1, M2, and M3," 406, 407,and 408, respectively, were monitored. Cell media (20 μL aliquot) was also sampled and processed to determine enrichment of glucose secreted into the media. Fractional glucose synthesis, "gluconeogenesis" was calculated by measuring the percentage of ^{13}C-enrichment (^{13}C-label incorporated into a glucose molecule as M2) or ^{2}H-enrichment (^{2}H-label incorporated into a glucose molecule as M2) and then dividing M2 ^{13}C-enrichment or ^{2}H-enrichment over MO, and the data were expressed as the percentage of fractional synthesis by multiplying by 100.

Statistics

Data are presented as mean ± SEM. Measurements were compared using an unpaired Student *t*-test with Welch's correction. Analysis of body weight, insulin level, glucose level, and HOMA in the congenic panels was based on the sequential analysis method as previously described (Shao et al. 2008, 2010; Millward et al. 2009). Briefly, each congenic strain was compared to the most genetically similar congenic strain with phenotypic differences (after Bonferoni correction for multiple hypothesis testing) attributed to sequence variation within the regions of DNA sequence that differ between the two strains. The sequential method of congenic strain analysis has numerous advantages over the "common-segment" method, including considerable improvements for resolving phenotypic heterogeneity and identifying novel QTLs (Shao et al. 2010). In particular, QTLs are found that account for phenotypic differences between overlapping congenic strains, even though some of those strains do not differ from B6. These QTLs show high statistical confidence and are highly reproducible. The QTLs identified in these studies have been drawn with their intervals arbitrarily extending halfway between the nearest flanking markers. However, the maximum possible QTL intervals, given the imperfect resolution of the defining recombination breakpoints, were assumed for all analyses.

Acknowledgments

This research was supported by the NIH NCRR grant RR12305, the NIH NCI Transdisciplinary Research on Energetics and Cancer (TREC) grant U54 CA116867, the NIH NHLBI grant F32-HL-82213, the NIH training grant T32-GM07250-30 to the Case MSTP (Medical Scientist Training Program), and NIDDK grant DK76169 for the CWRU MMPC (Mouse Metabolic Phenotyping Center). We also thank Jonathan Phan and Michael Morgan for assistance with genotyping and Dr. H. Brunengraber (director) for providing access to the CWRU MMPC.

References

Altshuler D, Daly MJ, Lander ES. 2008. Genetic mapping in human disease. *Science* **322:** 881–888.

Arya R, Blangero J, Williams K, Almasy L, Dyer TD, Leach RJ, O'Connell P, Stern MP, Duggirala R. 2002. Factors of insulin resistance syndrome–related phenotypes are linked to genetic locations on chromosomes 6 and 7 in nondiabetic Mexican-Americans. *Diabetes* **51:** 841–847.

Ashikov A, Routier F, Fuhlrott J, Helmus Y, Wild M, Gerardy-Schahn R, Bakker H. 2005. The human solute carrier gene SLC35B4 encodes a bifunctional nucleotide sugar transporter with specificity for UDP-xylose and UDP-N-acetylglucosamine. *J Biol Chem* **280:** 27230–27235.

Ayala JE, Bracy DP, McGuinness OP, Wasserman DH. 2006. Considerations in the design of hyperinsulinemic-euglycemic clamps in the conscious mouse. *Diabetes* **55:** 390–397.

Aylor DL, Valdar W, Foulds-Mathes W, Buus RJ, Verdugo RA, Baric RS, Ferris MT, Frelinger JA, Heise M, Frieman MB, et al. 2011. Genetic analysis of complext traits in the emerging collaborative cross. *Genome Res* (in press). doi: 10.1101/gr.111310.110.

Brown KM, MacGregor S, Montgomery GW, Craig DW, Zhao ZZ, Iyadurai KK, Henders A, Homer N, Campbel, MJ, Stark M, et al. 2008. Common sequence variants on 20q11.22 confer melanoma susceptibility. *Nat Genet* **40:** 838–840.

Brunetti-Pierri N, Berg JS, Scaglia F, Belmont J, Bacino CA, Sahoo T, Lalani SR, Graham B, Lee B, Shinawi M, et al. 2008. Recurrent reciprocal 1q21.1 deletions and duplications associated with microcephaly or macrocephaly and developmental and behavioral abnormalities. *Nat Genet* **40:** 1466–1471.

Buchner DA, Burrage LC, Hill AE, Yazbek SN, O'Brien WE, Croniger CM, Nadeau JH. 2008. Resistance to diet-induced obesity in mice with a single substituted chromosome. *Physiol Genomics* **35:** 116–122.

Buchner DA, Yazbek SN, Solinas P, Burrage LC, Morgan MG, Hoppel CL, Nadeau JH. 2010. Increased mitochondrial oxidative phosphorylation in the liver is associated with obesity and insulin resistance. *Obesity (Silver Spring)* **19:** 917–924.

Burrage L, Baskin-Hill A, Sinasac D, Singer J, Croniger C, Kirby A, Kulbokas E, Daly M, Lander E, Broman K, et al. 2010. Genetic resistance to diet-induced obesity in chromosome substitution strains of mice. *Mamm Genome* **21:** 115–129.

Cecil JE, Tavendale R, Watt P, Hetherington MM, Palmer CNA. 2008. An obesity-associated FTO gene variant and increased energy intake in children. *N Engl J Med* **359:** 2558–2566.

Cunningham F, Rios D, Griffiths M, Smith J, Ning Z, Cox T, Flicek P, Marin-Garcin P, Herrero J, Rogers J, et al. 2006. TranscriptSNPView: a genome-wide catalog of mouse coding variation. *Nat Genet* **38:** 853.

Di Bernardo MC, Crowther-Swanepoel D, Broderick P, Webb E, Sellick G, Wild R, Sullivan K, Vijayakrishnan J, Wang Y, Pittman AM, et al. 2008. A genome-wide association study identifies six susceptibility loci for chronic lymphocytic leukemia. *Nat Genet* **40:** 1204–1210.

Ehrenreich IM, Torabi N, Jia Y, Kent J, Martis S, Shapiro JA, Gresham D, Caudy AA, Kruglyak L. 2010. Dissection of genetically complex traits with extremely large pools of yeast segregants. *Nature* **464:** 1039–1042.

Emison ES, McCallion AS, Kashuk CS, Bush RT, Grice E, Lin S, Portnoy ME, Cutler DJ, Green ED, Chakravarti A. 2005. A common sex-dependent mutation in a RET enhancer underlies Hirschsprung disease risk. *Nature* **434:** 857–863.

Erkko H, Xia B, Nikkila J, Schleutker J, Syrjakoski K, Mannermaa A, Kallioniemi A, Pylkas K, Karppinen SM, Rapakko K, et al. 2007. A recurrent mutation in PALB2 in Finnish cancer families. *Nature* **446:** 316–319.

Feitosa MF, Borecki IB, Rich SS, Arnett DK, Sholinsky P, Myers RH, Leppert M, Province MA. 2002. Quantitative-trait loci influencing body-mass index reside on chromosomes 7 and 13: the National Heart, Lung, and Blood Institute Family Heart Study. *Am J Hum Genet* **70:** 72–82.

Flint J, Mackay TF. 2009. Genetic architecture of quantitative traits in mice, flies, and humans. *Genome Res* **19:** 723–733.

Fox CS, Heard-Costa N, Cupples LA, Dupuis J, Vasan RS, Atwood LD. 2007. Genome-wide association to body mass index and waist circumference: the Framingham Heart Study 100K project. *BMC Med Genet* **8** (Suppl 1) : S18. doi: 10.1186/1471-2350-8-S1-S18.

Gerken T, Girard CA, Tung Y-CL, Webby CJ, Saudek V, Hewitson KS, Yeo GSH, McDonough MA, Cunliffe S, McNeill LA, et al. 2007. The obesity-associated FTO gene encodes a 2-oxoglutarate-dependent nucleic acid demethylase. *Science* **318:** 1469–1472.

Gibson G. 2009. Decanalization and the origin of complex disease. *Nat Rev Genet* **10:** 134–140.

Goldstein DB. 2009. Common genetic variation and human traits. *N Engl J Med* **360:** 1696–1698.

Halseth AE, Bracy DP, Wasserman DH. 1999. Overexpression of hexokinase II increases insulinand exercise-stimulated muscle glucose uptake in vivo. *Am J Physiol* **276:** E70–E77.

Hill-Baskin AE, Markiewski MM, Buchner DA, Shao H, DeSantis D, Hsiao G, Subramaniam S, Berger NA, Croniger C, Lambris JD, et al. 2009. Diet-induced hepatocellular carcinoma in genetically predisposed mice. *Hum Mol Genet* **18:** 2975–2988.

Inoue M, Chiang SH, Chang L, Chen XW, Saltiel AR. 2006. Compartmentalization of the exocyst complex in lipid rafts controls Glut4 vesicle tethering. *Mol Biol Cell* **17:** 2303–2311.

Kruglyak L. 2008. The road to genome-wide association studies. *Nat Rev Genet* **9:** 314–318.
Laramie JM, Wilk JB, Williamson SL, Nagle MW, Latourelle JC, Tobin JE, Province MA, Borecki IB, Myers RH. 2008. Polymorphisms near EXOC4 and LRGUK on chromosome 7q32 are associated with type 2 diabetes and fasting glucose: the NHLBI Family Heart Study. *BMC Med Genet* **9:** 46.
Love DC, Hanover JA. 2005. The hexosamine signaling pathway: deciphering the "O-GlcNAc code". *Sci STKE* **2005:** re13. doi: 10.1126/stke.3122005re13.
Lyons PD, Peck GR, Kettenbach AN, Gerber SA, Roudaia L, Lienhard GE. 2009. Insulin stimulates the phosphorylation of the exocyst protein Sec8 in adipocytes. *Biosci Rep* **29:** 229–235.
Mackay TFC, Stone EA, Ayroles JF. 2009. The genetics of quantitative traits: challenges and prospects. *Nat Rev Genet* **10:** 565–577.
Manolio TA, Collins FS, Cox NJ, Goldstein DB, Hindorff LA, Hunter DJ, McCarthy MI, Ramos EM, Cardon LR, Chakravarti A, et al. 2009. Finding the missing heritability of complex diseases. *Nature* **461:** 747–753.
Matin A, Collin GB, Asada Y, Varnum D, Nadeau JH. 1999. Susceptibility to testicular germ-cell tumours in a 129.MOLF-Chr 19 chromosome substitution strain. *Nat Genet* **23:** 237–240.
McClellan J, King M-C. 2010. Genetic heterogeneity in human disease. *Cell* **141:** 210–217.
Meijers-Heijboer H, van den Ouweland A, Klijn J, Wasielewski M, de Snoo A, Oldenburg R, Hollestelle A, Houben M, Crepin E, van Veghel-Plandsoen M, et al. 2002. Low-penetrance susceptibility to breast cancer due to CHEK2(*)1100delC in noncarriers of BRCA1 or BRCA2 mutations. *Nat Genet* **31:** 55–59.
Millward CA, Burrage LC, Shao H, Sinasac DS, Kawasoe JH, Hill-Baskin AE, Ernest SR, Gornicka A, Hsieh CW, Pisano S, et al. 2009. Genetic factors for resistance to diet-induced obesity and associated metabolic traits on mouse chromosome 17. *Mamm Genome* **20:** 71–82.
Mott R, Flint J. 2008. Prospects for complex trait analysis in the mouse. *Mamm Genome* **19:** 306–308.
Nadeau JH. 2009. Transgenerational genetic effects on phenotypic variation and disease risk. *Hum Mol Genet* **18:** R202–R210.
Nadeau JH, Singer JB, Matin A, Lander ES. 2000. Analysing complex genetic traits with chromosome substitution strains. *Nat Genet* **24:** 221–225.
Papaemmanuil E, Hosking FJ, Vijayakrishnan J, Price A, Olver B, Sheridan E, Kinsey SE, Lightfoot T, Roman E, Irving JA, et al. 2009. Loci on 7p12.2, 10q21.2 and 14q11.2 are associated with risk of childhood acute lymphoblastic leukemia. *Nat Genet* **41:** 1006–1010.
Phillips PC. 2008. Epistasis: the essential role of gene interactions in the structure and evolution of genetic systems. *Nat Rev Genet* **9:** 855–867.
Plank J, Blaha J, Cordingley J, Wilinska ME, Chassin LJ, Morgan C, Squire S, Haluzik M, Kremen J, Svacina S, et al. 2006. Multicentric, randomized, controlled trial to evaluate blood glucose control by the model predictive control algorithm versus routine glucose management protocols in intensive care unit patients: Response to Ligtenberg et al. *Diabetes Care* **29:** 1987–1988.
Previs SF, Ciraolo ST, Fernandez CA, Beylot M, Agarwal KC, Soloview MV, Brunengraber H. 1994. Use of [6,6-2H2]glucose and of low-enrichment [U-13C6]-glucose for sequential or simultaneous measurements of glucose turnover by gas chromatography-mass spectrometry. *Anal Biochem* **218:** 192–196.
Rahman N, Seal S, Thompson D, Kelly P, Renwick A, Elliott A, Reid S, Spanova K, Barfoot R, Chagtai T, et al. 2007. PALB2, which encodes a BRCA2-interacting protein, is a breast cancer susceptibility gene. *Nat Genet* **39:** 165–167.
Renwick A, Thompson D, Seal S, Kelly P, Chagtai T, Ahmed M, North B, Jayatilake H, Barfoot R, Spanova K, et al. 2006. ATM mutations that cause ataxia-telangiectasia are breast cancer susceptibility alleles. *Nat Genet* **38:** 873–875.
Saito T, Shibasaki T, Seino S. 2008. Involvement of Exoc3l, a protein structurally related to the exocyst subunit Sec6, in insulin secretion. *Biomed Res* **29:** 85–91.
Saunders CL, Chiodini BD, Sham P, Lewis CM, Abkevich V, Adeyemo AA, de Andrade M, Arya R, Berenson GS, Blangero J, et al. 2007. Meta-analysis of genome-wide linkage studies in BMI and obesity. *Obesity (Silver Spring)* **15:** 2263–2275.
Seal S, Thompson D, Renwick A, Elliott A, Kelly P, Barfoot R, Chagtai T, Jayatilake H, Ahmed M, Spanova K, et al. 2006. Truncating mutations in the Fanconi anemia J gene BRIP1 are low-penetrance breast cancer susceptibility alleles. *Nat Genet* **38:** 1239–1241.
Shao H, Burrage LC, Sinasac DS, Hill AE, Ernest SR, O'Brien W, Courtland HW, Jepsen KJ, Kirby A, Kulbokas EJ, et al. 2008. Genetic architecture of complex traits: large phenotypic effects and pervasive epistasis. *Proc Natl Acad Sci* **105:** 19910–19914.
Shao H, Sinasac DS, Burrage LC, Hodges CA, Supelak PJ, Palmert MR, Moreno C, Cowley MA, Jacob HJ, Nadeau JH. 2010. Analyzing complex traits with congenic strains. *Mamm Genome* **21:** 276–286.
Siepel A, Bejerano G, Pedersen JS, Hinrichs AS, Hou M, Rosenbloom K, Clawson H, Spieth J, Hillier LW, Richards S, et al. 2005. Evolutionarily conserved elements in vertebrate, insect, worm, and yeast genomes. *Genome Res* **15:** 1034–1050.
Singer JB, Hill AE, Burrage LC, Olszens KR, Song J, Justice M, O'Brien WE, Conti DV, Witte JS, Lander ES, et al. 2004. Genetic dissection of complex traits with chromosome substitution strains of mice. *Science* **304:** 445–448.
Stolerman ES, Florez JC. 2009. Genomics of type 2 diabetes mellitus: implications for the clinician. *Nat Rev Endocrinol* **5:** 429–436.
Tang W, Miller MB, Rich SS, North KE, Pankow JS, Borecki IB, Myers RH, Hopkins PN, Leppert M, Arnett DK. 2003. Linkage analysis of a composite factor for the multiple metabolic syndrome: the National Heart, Lung, and Blood Institute Family Heart Study. *Diabetes* **52:** 2840–2847.
Teo CF, Wollaston-Hayden EE, Wells L. 2010. Hexosamine flux, the O-GlcNAc modification, and the development of insulin resistance in adipocytes. *Mol Cell Endocrinol* **318:** 44–53.
Tomlinson IPM, Webb E, Carvajal-Carmona L, Broderick P, Howarth K, Pittman AM, Spain S, Lubbe S, Walther A, Sullivan K, et al. 2008. A genome-wide association study identifies colorectal cancer susceptibility loci on chromosomes 10p14 and 8q23.3. *Nat Genet* **40:** 623–630.
Wahlsten D, Metten P, Phillips TJ, Boehm SL II, Berkhart-Kasch S, Dorow J, Doerksen S, Downing C, Fogarty J, Rodd-Henricks K, et al. 2003. Different data from different labs: Lessons from studies of gene-environment interaction. *J Neurobiol* **54:** 283–311.
Wu C, Orozco C, Boyer J, Leglise M, Goodale J, Batalov S, Hodge CL, Haase J, Janes J, Huss JW 3rd, et al. 2009. BioGPS: an extensible and customizable portal for querying and organizing gene annotation resources. *Genome Biol* **10:** R130. doi: 10.1186/gb-2009-10-11-r130.
Yang X, Ongusaha PP, Miles PD, Havstad JC, Zhang F, So WV, Kudlow JE, Michell RH, Olefsky JM, Field SJ, et al. 2008. Phosphoinositide signalling links O-GlcNAc transferase to insulin resistance. *Nature* **451:** 964–969.
Youngren KK, Nadeau JH, Matin A. 2003. Testicular cancer susceptibility in the 129.MOLF-Chr19 mouse strain: additive effects, gene interactions and epigenetic modifications. *Hum Mol Genet* **12:** 389–398.

Received January 13, 2011; accepted in revised form April 12, 2011.